

# The influence of hydrophobic substitution on self-association of poly(ethylene oxide)-*b*-poly(*n*-alkyl glycidyl carbamate)s-*b*-poly(ethylene oxide) triblock copolymers in aqueous media

Philip Dimitrov<sup>a,1</sup>, Maria Jamróz-Piegza<sup>a</sup>, Barbara Trzebicka<sup>a</sup>, Andrzej Dworak<sup>a,b,\*</sup>

<sup>a</sup> Institute of Coal Chemistry, Polish Academy of Sciences, ul. Sowińskiego 5, 44-121 Gliwice, Poland

<sup>b</sup> University of Opole, Institute of Chemistry, ul. Oleska 48, 45-052 Opole, Poland

Received 14 October 2006; received in revised form 25 January 2007; accepted 9 February 2007

Available online 14 February 2007

## Abstract

A series of amphiphilic poly(ethylene oxide)-*b*-poly(*n*-alkyl glycidyl carbamate)s-*b*-poly(ethylene oxide) triblock copolymers were synthesized by reaction between poly(ethylene oxide)-*b*-polyglycidol-*b*-poly(ethylene oxide) precursor copolymer and four *n*-alkyl isocyanates: ethyl, propyl, butyl and pentyl. After dissolution in water at room temperature the copolymers spontaneously form micelles. The critical micellization concentrations were determined by UV–VIS spectroscopy. The dimensions of the micelles, the aggregation numbers, and in some cases the micellar shape were determined by dynamic and static light scattering in a relatively broad temperature range. Special attention has been paid to the influence of the number of the carbon atoms in the alkyl chains, and respectively, the relative hydrophobicity of the middle block upon the self-association process. Clouding transition was observed for all of the copolymers, the clouding point being dependent upon the length of the alkyl chain.

© 2007 Elsevier Ltd. All rights reserved.

**Keywords:** Amphiphilic block copolyethers; Self-association; Micelles

## 1. Introduction

The self-assembly of amphiphilic block copolymers in aqueous media is a predominantly entropy controlled process which can result in the formation of highly ordered supramolecular structures. In the majority of cases fairly well defined micelles of different morphology [1], vesicles [2] and liquid crystalline phases [3] are being formed. Polymeric micelles are of special interest due to their potential application in advanced drug delivery systems [4], templates for nanoporous materials [5], nanoparticles [6] and many others. The

relationship between block copolymer composition and the resulting supramolecular aggregates has been thoroughly investigated during last two decades [7,8]. As a common rule in most of the systems, the length of the hydrophobic blocks, or the corresponding hydrophobicity, is one of the most important factors for the self-association. The length of the hydrophobic block directly influences important parameters such as critical micellization concentration (cmc), the aggregation number ( $N_{agg}$ ), the radius of gyration ( $R_g$ ), the hydrodynamic radius ( $R_h$ ), etc. Block copolymers with longer hydrophobic blocks exhibit lower critical micellization concentration, and typically higher aggregation number and larger dimensions [9]. Special attention has been paid to the influence of the linear architecture of the block copolymers (AB, ABA, and BAB), where the letter A usually stands for the water-soluble moiety, which in many cases is poly(ethylene oxide) (PEO), and B stands for various hydrophobic blocks such as polyoxyalkylenes, polystyrene, and many others [7,9].

\* Corresponding author. Institute of Coal Chemistry, Polish Academy of Sciences, ul. Sowińskiego 5, 44-121 Gliwice, Poland. Tel.: +48 32 2380780; fax: +48 32 2312831.

E-mail address: [adworak@karboch.gliwice.pl](mailto:adworak@karboch.gliwice.pl) (A. Dworak).

<sup>1</sup> On leave from Institute of Polymers, Bulgarian Academy of Sciences, Sofia, Bulgaria.

In the simplest case of AB diblock copolymers two basic types of micellar structures are known to be formed depending on the relative length of the hydrophobic block. “Star-like” micelles having highly swollen shells are formed if the hydrophilic block is larger than the hydrophobic [10]; in the case of a short shell-forming block “crew-cut” micelles with large cores were observed [11]. Crew-cut aggregates are also known to exist in versatile shapes depending on the environmental conditions as demonstrated by the group of Eisenberg [12]. ABA copolymers can form spherical core-shell micelles which are similar to diblock copolymers’ micelles [13]. The cmc of these copolymers depends both upon the length and the nature of the hydrophobic block: the longer the hydrophobic block, the lower the cmc. The hydrophobic blocks decrease the cmc of copolymers in following order of monomeric units of increasing hydrophobicity: propylene oxide,  $\epsilon$ -caprolactone, alkyl chain, butylenes oxide and styrene oxide [8,10,14,15].

The self-organization of the amphiphilic copolymers containing poly(ethylene oxide) block as the hydrophilic sequence has been extensively studied, because of the numerous potential and actual applications of PEO due to its biocompatibility, protein resistance [16], lack of immunogenicity and rapid clearance from the human body [17]. Many properties were investigated. Both radius of gyration and hydrodynamic radius of the micelles formed by these copolymers increase with the length of PEO block.

It was also observed that the aggregation number and the hydrodynamic radii of poly(ethylene oxide)-based copolymers increases with temperature [9,18,19].

Here we report the results of the study of the micellization of well defined triblock copolymers of poly(ethylene oxide)-*b*-poly(*n*-alkyl glycidyl carbamate)-*b*-poly(ethylene oxide). The DP of the PEO blocks is 108 and the DP of the hydrophobic block is 38 for all copolymers. The molar mass distribution is narrow ( $M_w/M_n < 1.03$ ). The only factor changed is the length of the *n*-alkyl substituent in the hydrophobic block: ethyl, *n*-propyl, *n*-butyl and *n*-pentyl were used. This narrowing of structural variables is expected to clarify the influence of the hydrophobicity upon the association behaviour.

## 2. Experimental

### 2.1. Materials

All solvents were purified by standard methods. *t*-BuOK 97.0% (Aldrich), dibutyltin dilaurate 95% (DBTL) (Aldrich), *n*-propyl isocyanate 99.0% (Aldrich), *n*-butyl isocyanate 98.0% (Aldrich) and *n*-pentyl isocyanate 98.0% (Acros Organics) were used as received. Diethylene glycol (Aldrich) was distilled under reduced pressure prior to use. Ethoxyethyl glycidyl ether (EEGE) was obtained by reacting 2,3-epoxypropanol-1(glycidol) with ethyl vinyl ether according to procedure described by Fitton et al. [20]. The obtained product was fractionated under reduced pressure. Fractions of purity exceeding 99.8% (GC) were used for polymerization. Ethylene oxide (Aldrich) was kept over CaH<sub>2</sub> and distilled prior to polymerization. DMF (POCH Gliwice) was dried over

CaH<sub>2</sub>, distilled, then dried over P<sub>2</sub>O<sub>5</sub> and distilled again. Ethyl isocyanate 98.0% (Aldrich) was distilled under nitrogen atmosphere.

### 2.2. Synthesis and modification of block copolymers

The synthesis of the precursor block copolymer poly(ethylene oxide)-*b*-polyglycidol-*b*-poly(ethylene oxide) EO<sub>108</sub>G<sub>38</sub>EO<sub>108</sub> and its characteristics have been described in detail in a previous work [21]. First, the triblock copolymer EO<sub>108</sub>EEGE<sub>38</sub>EO<sub>108</sub> was obtained by sequential anionic polymerization of EEGE and EO initiated by potassium diethyleneglycolate. EO<sub>108</sub>G<sub>38</sub>EO<sub>108</sub> block copolymer was obtained after acidic cleavage of the ethoxyethyl groups from the EEGE units. After purification by dialysis against deionised water followed by drying under reduced pressure, EO<sub>108</sub>G<sub>38</sub>EO<sub>108</sub> block copolymer was dissolved in dry DMF (150 g/L) under nitrogen atmosphere and reacted with ethyl (Et), *n*-propyl (Pr), *n*-butyl (Bu) and *n*-pentyl (Pn) isocyanate in presence of DBTL as a catalyst. The molar ratio [glycidol units]:[*n*-alkyl isocyanate]:[DBTL] was 1:2:0.02. The reaction was carried out at 40 °C for 48 h. After the removal of DMF, the reaction product was dissolved in methylene chloride and precipitated into diethyl ether cooled to –10 °C. After three precipitations the product was dried under reduced pressure. Four copolymers of common composition EO<sub>108</sub>AGC<sub>38</sub>EO<sub>108</sub>, where A stands for ethyl (Et), *n*-propyl (Pr), *n*-butyl (Bu), or *n*-pentyl (Pn), were obtained.

### 2.3. Characterization of block copolymers

The <sup>1</sup>H NMR spectra were recorded at 25 °C on a Varian Unity-Inova spectrometer operating at 300 MHz and using CDCl<sub>3</sub> as a solvent.

SEC measurements of the copolymers were made on a setup of four PSS SDV columns of nominal pore sizes 1 × 10<sup>5</sup>, 1 × 1000, 2 × 100 Å, a differential refractive index detector Δ*n*-1000 RI WGE DR Bures and a multiangle laser light scattering (MALLS) detector DAWN EOS from Wyatt Technologies. THF was used as the eluent at 35 °C with a nominal flow rate of 1 mL/min. The specific refractive index increment (dn/dc) of polymer samples in THF was measured at 35 °C using a Δ*n*-1000 RI WGE DR Bures differential refractive index detector. SEC results were put together and evaluated by ASTRA IV software from Wyatt Technologies.

### 2.4. Preparation of micellar solutions

Micelles from EO<sub>108</sub>AGC<sub>38</sub>EO<sub>108</sub> copolymers were prepared by direct dissolution in deionised water (Hydrolab HLP5 deionisator) filtered through 0.02 μm Whatman ANOTOP membrane. To achieve a faster equilibration solutions were heated to 60 °C, and then cooled down to room temperature. An initial stock solution of 20 g/L was diluted in order to obtain series of solutions with concentrations reaching down to 0.01 g/L. To remove possible dust impurities

the micellar dispersions were filtered through 0.1  $\mu\text{m}$  Whatman PURADISC syringe filters.

### 2.5. Cloud point measurements

Cloud points of 5 g/L aqueous copolymer solutions were determined on a Jasco V-530 UV–VIS spectrophotometer switched to transmittance regime at constant wavelength of 500 nm. The cuvette compartment was thermostated by Medson MTC-P1 thermocontroller with a stability of  $\pm 0.05$  °C. Cloud points were determined from the maxima of the first derivative of transmittance against temperature curves.

### 2.6. Hydrophobic dye solubilization

Aqueous solutions (3 mL) of a block copolymer in the concentration range from 0.01 to 10 g/L were prepared as described above. Thirty microlitres of a 0.4 mM solution of 1,6-diphenyl-1,3,5-hexatriene (DPH) in methanol were added to each of the copolymer solutions. Solutions were incubated in the dark for 16 h at room temperature. The absorbance in the range of  $\lambda = 300$ –500 nm was followed on a Jasco V-530 UV–VIS spectrophotometer at temperatures of 25 and 40 °C. Before recording the spectra, the samples were thermostated for 10 min, after which the intensity of the characteristic absorption peak at 356 nm for DPH solubilized in a hydrophobic domain [14] remained constant.

### 2.7. Dynamic light scattering

DLS measurements were performed on a Brookhaven BI-200 goniometer with vertically polarized incident light of wavelength  $\lambda = 632.8$  nm supplied by a helium–neon laser operated at 75 mW and a Brookhaven BI-9000 AT digital autocorrelator. Measurements of scattered light from the polymer aqueous solutions were made at angles  $\theta$  from 40° to 140° to the incident beam in temperature range from 25 to 70 °C. The autocorrelation functions from DLS were analysed by the constrained regularized CONTIN method [27] to obtain distributions of decay rates ( $\Gamma$ ). The decay rates gave the apparent diffusion coefficients  $D = \Gamma/q^2$ , where  $q$  is the magnitude of the scattering vector  $q = (4\pi n/\lambda)\sin^2(\theta/2)$ . The mean hydrodynamic radii were obtained by the Stokes–Einstein equation:

$$R_h = kT/(6\pi\eta D_0) \quad (1)$$

where  $k$  is the Boltzmann constant,  $\eta$  is the viscosity of water at temperature  $T$  and  $D_0$  is the diffusion coefficient at infinite dilution.

### 2.8. Static light scattering

Static light scattering (SLS) measurements were carried out on the Brookhaven instrument described above at angles ranging from 40° to 140° to the incident beam at temperatures ranging from 25 to 70 °C. The SLS data analyses were

performed by the Zimm plot software provided from Brookhaven Instruments using the Rayleigh–Gans–Debye equation [22]:

$$\frac{Kc}{R_\theta} = \frac{1 + R_g^2 q^2/3}{\bar{M}_w} + 2A_2c \quad (2)$$

where  $K \equiv 4\pi^2 n_0^2 (dn/dc)^2 / N_A \lambda^4$  is an optical parameter with  $n_0$  being the refractive index of solvent,  $N_A$  is the Avogadro's constant,  $\lambda$  is the laser wavelength (632.8 nm);  $\bar{M}_w$  is the weight-average molar mass of the solute,  $A_2$  is the second virial coefficient,  $R_\theta$  is the Rayleigh ratio of the polymer solution at a given angle. The  $dn/dc$  values of the aqueous micellar solutions were determined on a  $\Delta n$ -1000 RI WGE Dr Bures differential refractive index detector.

$R_g$  values were also determined for single copolymer concentration of 5 g/L by partial Zimm plots, which are described by the following equation:

$$\frac{1}{I_{\text{ex}}} = C \left( 1 + \frac{R_g^2 q^2}{3} \right) \quad (3)$$

where  $I_{\text{ex}}$  is the excess of the scattered light.

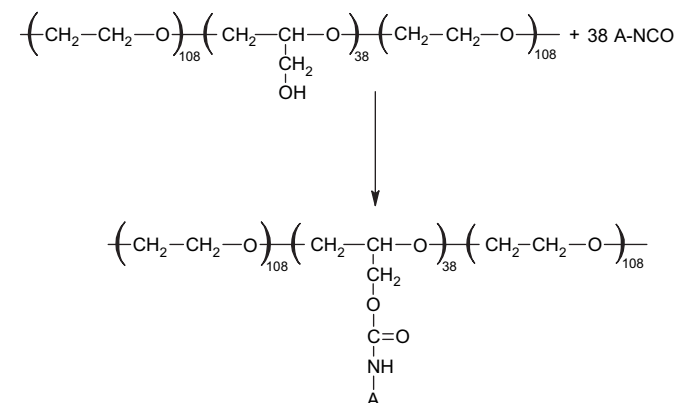
## 3. Results and discussion

### 3.1. Synthesis and characterization of block copolymers

The quantitative reaction of the primary hydroxyl groups from the central block of  $\text{EO}_{108}\text{G}_{38}\text{EO}_{108}$  precursor copolymer with ethyl, *n*-propyl, *n*-butyl or *n*-pentyl isocyanates gave the final poly(ethylene oxide)-*b*-poly(alkyl glycidyl carbamate)-*b*-poly(ethylene oxide) copolymers. The obtained copolymers differ only by the type of the hydrophobic monomer units, as shown in Scheme 1.

For each of the  $\text{EO}_{108}\text{AGC}_{38}\text{EO}_{108}$  copolymers the degree of substitution of the central polyglycidol block was near 100% as confirmed by the  $^1\text{H}$  NMR spectra (Fig. 1).

The molar mass characteristics of the synthesized four amphiphilic block copolymers are summarized in Table 1.



A = alkyl group = Et, Pr, Bu, Pn

Scheme 1. Synthesis of  $\text{EO}_{108}\text{AGC}_{38}\text{EO}_{108}$  amphiphilic block copolymers.

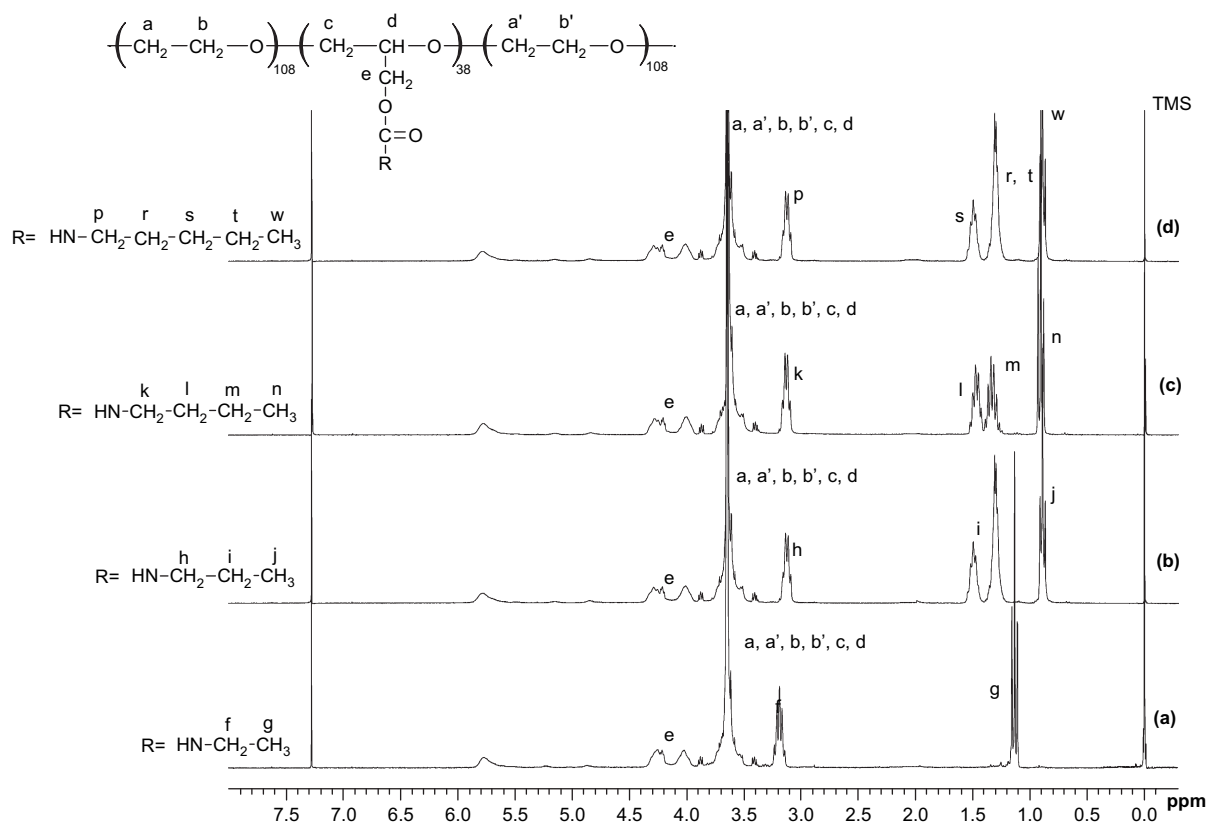


Fig. 1.  $^1\text{H}$  NMR spectra of (a)  $\text{EO}_{108}\text{EtGC}_{38}\text{EO}_{108}$ , (b)  $\text{EO}_{108}\text{PrGC}_{38}\text{EO}_{108}$ , (c)  $\text{EO}_{108}\text{BuGC}_{38}\text{EO}_{108}$ , and (d)  $\text{EO}_{108}\text{PnGC}_{38}\text{EO}_{108}$  amphiphilic block copolymers (300 MHz,  $\text{CDCl}_3$ ).

The results for the precursor are also included. The peaks obtained from the SEC analysis were narrow and symmetrical. Only a small tail at the low molar mass region of the chromatograms was observed for the starting  $\text{EO}_{108}\text{G}_{38}\text{EO}_{108}$  and the obtained amphiphilic block copolymers. In no case it made more than 5% of the total yield. As discussed previously [21] the low molecular impurities represent PEO-rich fractions, and therefore they are not of importance for self-association process of the block copolymers.

Molar masses of the obtained copolymers were determined from  $M_n$  of the starting block and copolymer composition measured by  $^1\text{H}$  NMR (2nd column in Table 1). They are in good agreement with the masses measured with

Table 1  
Composition and molar masses of  $\text{EO}_{108}\text{AGC}_{38}\text{EO}_{108}$  and  $\text{EO}_{108}\text{G}_{38}\text{EO}_{108}$  precursor

Sample	$M_n^a$ (calc.)	$M_n$ (SEC–MALLS)	$M_w/M_n$ (SEC–MALLS)	$dn/dc$ (in THF)
$\text{EO}_{108}\text{G}_{38}\text{EO}_{108}^b$	—	13 400	1.03	0.050
$\text{EO}_{108}\text{EtGC}_{38}\text{EO}_{108}$	15 500	15 000	1.02	0.069
$\text{EO}_{108}\text{PrGC}_{38}\text{EO}_{108}$	15 200	15 000	1.03	0.060
$\text{EO}_{108}\text{BuGC}_{38}\text{EO}_{108}$	15 700	16 000	1.02	0.058
$\text{EO}_{108}\text{PnGC}_{38}\text{EO}_{108}$	16 200	16 500	1.02	0.053

<sup>a</sup> From the molar mass of unsubstituted triblock copolymer and degree of substitution detected by  $^1\text{H}$  NMR.

<sup>b</sup> SEC–MALLS measurements were done in DMF/LiBr [21].

SEC–MALLS (to ensure accuracy, the refractive index increments for each copolymer were determined independently). The architecture of the studied copolymers, and the degrees of polymerization of the hydrophobic and the hydrophilic blocks of  $\text{EO}_{108}\text{AGC}_{38}\text{EO}_{108}$  are the same as of the commercially available amphiphilic block copolymer of EO and propylene oxide Pluronic F88 [23,24].

### 3.2. Cloud point measurements

All of the synthesized block copolymers exhibited clouding of their water solutions due to the lower critical solution temperature. Measurements of the clouding temperature were performed for 5 g/L solutions of copolymers in water, at concentrations higher than cmc values of the copolymers, thus favouring the intermolecular interactions of the macromolecules. Cloud point data are presented in Table 2. As shown in Fig. 2(a) the cloud point transitions were sharp and

Table 2  
Cloud point and cmc of  $\text{EO}_{108}\text{AGC}_{38}\text{EO}_{108}$  block copolymers

Composition	$T_{CP}^a$ (°C)	Cmc at 25 °C (g/L)	$X_{cmc} \times 10^6$ (mol fr.)
$\text{EO}_{108}\text{EtGC}_{38}\text{EO}_{108}$	86.4	2.5	3.00
$\text{EO}_{108}\text{PrGC}_{38}\text{EO}_{108}$	81.5	1.8	2.00
$\text{EO}_{108}\text{BuGC}_{38}\text{EO}_{108}$	71.5	1.0	1.08
$\text{EO}_{108}\text{PnGC}_{38}\text{EO}_{108}$	61.9	0.6	0.62

<sup>a</sup> For 5 g/L solutions.

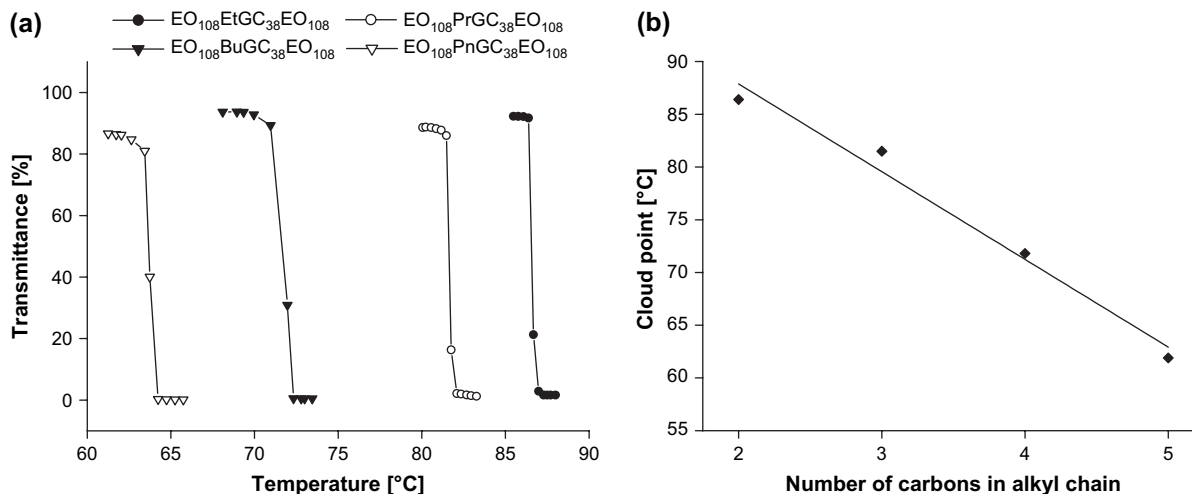


Fig. 2. (a) Transmittance of 5 g/L aqueous solutions of the block copolymers at 500 nm versus temperature; (b) cloud point temperature as a function of number of carbons in the alkyl side group.

depended almost linearly on the length of the alkyl group in the alkyl glycidyl carbamate units (Fig. 2(b)) – the longer the alkyl group, the lower the cloud points observed. Provided that the longer alkyl groups give higher hydrophobicity of the macromolecules, this tendency is in line with the other findings for polyether amphiphilic block copolymer systems [9].

### 3.3. Cmc measurements

Critical micellization concentrations of the EO<sub>108</sub>AGC<sub>38</sub>EO<sub>108</sub> copolymers were determined by the hydrophobic dye (DPH) solubilization method, which is based on the ability of DPH molecules to absorb light only when placed in hydrophobic domains, i.e. micelle cores [14]. The measurements were performed at different temperatures. Cmc values were obtained as shown in Fig. 3. Similar to recently investigated block copolymers of EO and ethyl glycidyl carbamate [21], the cmc values of EO<sub>108</sub>AGC<sub>38</sub>EO<sub>108</sub> did not change significantly with temperature. Results obtained at 25 °C are summarized in Table 2. The cmc values decreased with increasing the

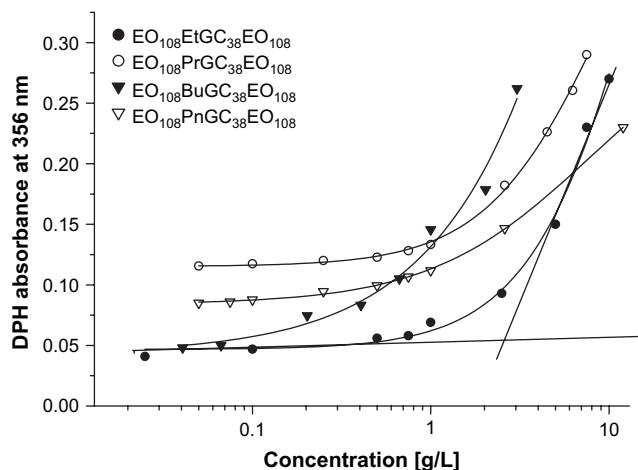


Fig. 3. Cmc curves for copolymers EO<sub>108</sub>AGC<sub>38</sub>EO<sub>108</sub> obtained at 25 °C.

hydrophobicity of the central block with respect to the increasing length of the *n*-alkyl groups.

### 3.4. Dynamic light scattering

Dynamic light scattering from micellar aqueous solutions was performed in the angular region from 40° to 140°. The hydrodynamic radii ( $R_h$ ) of the copolymer micelles were determined at different temperatures using Eq. (1) and  $D_0$  values obtained after extrapolation of diffusion coefficients for different concentrations to zero concentration. An example is given in Fig. 4.

The distributions of the intensity of the light scattered from the obtained micelles were monomodal from 25 to 60 °C except for EO<sub>108</sub>EtGC<sub>38</sub>EO<sub>108</sub>. As it was shown previously [21] at 25 °C aqueous solutions of EO<sub>108</sub>EtGC<sub>38</sub>EO<sub>108</sub> displayed bimodal distribution. Micelles of  $R_h$  equal to 3.6 nm coexist with much larger loose aggregates of non-micellar structure. The formation of large aggregates was explained to be caused by hydrogen bonding engaging water molecules and carbamate groups of central copolymer blocks [21]. With increasing the temperature the large aggregates disappear and the system becomes populated with micelles of larger hydrodynamic radii (Table 3). For the investigated copolymers the hydrophobicity of the chain is controlled and increases with the length of the *n*-alkyl chain of the carbamate groups. The increased hydrophobicity of the central blocks in the case of Pr, Bu and Pn seemed to prevent the formation of large aggregates. In these cases the hydrophobic effect is clearly controlling the system and the formation of hydrogen bonds appears to be less favourable process.

The temperature does not influence significantly the  $R_h$  values of EO<sub>108</sub>AGC<sub>38</sub>EO<sub>108</sub> micelles (Fig. 5(a) and Table 3). Micelles of EO<sub>108</sub>EtGC<sub>38</sub>EO<sub>108</sub> slightly increase their  $R_h$  from 3.6 nm at 25 °C to 7.4 nm at 60 °C. Micelles of EO<sub>108</sub>PrGC<sub>38</sub>EO<sub>108</sub> were the most stable compared to the other homologs, having  $R_h$  of 8–9 nm in the whole



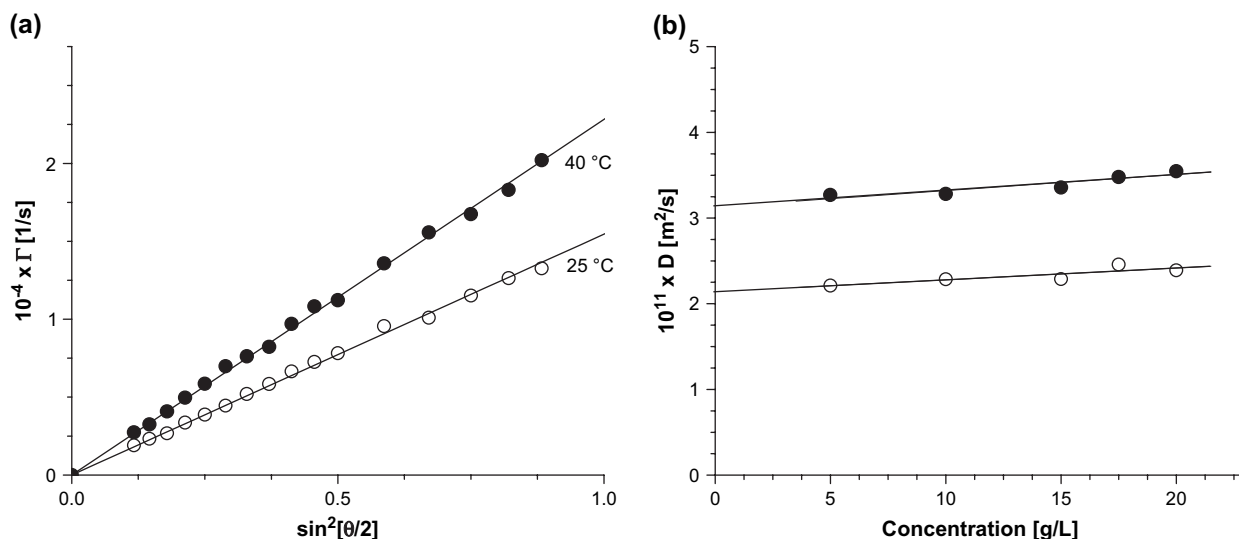


Fig. 4. (a) Relaxation rate ( $I$ ) as a function of  $\sin^2(\theta/2)$  for 5 g/L aqueous solution of  $\text{EO}_{108}\text{BuGC}_{38}\text{EO}_{108}$  at 25 (hollow circles), and at 40 °C (black circles); (b) concentration dependence of apparent diffusion coefficients for  $\text{EO}_{108}\text{BuGC}_{38}\text{EO}_{108}$  micelles at 25 °C (hollow circles) and at 40 °C (black circles). The lines through the points are linear fits.

temperature interval. As best seen in Fig. 5(a),  $R_h$  of the last two and most hydrophobic homologs,  $\text{EO}_{108}\text{BuGC}_{38}\text{EO}_{108}$  and  $\text{EO}_{108}\text{PnGC}_{38}\text{EO}_{108}$ , tend to decrease very slightly with increasing temperature. The hydrodynamic radii of the  $\text{EO}_{108}\text{AGC}_{38}\text{EO}_{108}$  micelles regularly increased with the increasing number of carbons in the pendant  $n$ -alkyl groups from the middle block (Fig. 5(b) and Table 3).

### 3.5. Static light scattering

SLS measurements were performed for  $\text{EO}_{108}\text{AGC}_{38}\text{EO}_{108}$  at copolymer concentrations above the cmc values at several temperatures where the distribution of the particle sizes

observed by DLS was monomodal. The  $R_g$  of  $\text{EO}_{108}\text{AGC}_{38}\text{EO}_{108}$  block copolymer micelles was obtained at 25 and 40 °C either from Zimm plots (an example for  $\text{EO}_{108}\text{PnGC}_{38}\text{EO}_{108}$  is shown in Fig. 6(a)) or from partial Zimm plots (Eq. (3)) for 5 g/L solution at higher temperatures as shown for  $\text{EO}_{108}\text{PnGC}_{38}\text{EO}_{108}$  (Fig. 6(b)). For all copolymers the corresponding weight-average molar masses of the micelles,  $\overline{M}_w^{\text{mic}}$ , and the radii of gyration,  $R_g$ , for structures of  $R_g > 15$  nm, were obtained. For the calculation of molar masses at different temperatures the  $dn/dc$  values measured at 35 °C were used. It was previously shown [21] that for polyether-based block copolymers  $dn/dc$  values change only slightly with temperature and therefore the obtained molar masses were believed to be consistent and close to the real ones.

The values of micelle sizes obtained from SLS and DLS measurements are presented in Table 3.

The weight-average aggregation number  $N_{\text{agg}}$  of the micelles was obtained from the following relationship:

$$N_{\text{agg}} = \overline{M}_w^{\text{mic}} / \overline{M}_w^{\text{uni}} \quad (4)$$

where  $\overline{M}_w^{\text{uni}}$  is the weight-average molar mass of the unimers (Table 1).

SLS results are summarized in Table 4.

With the increasing number of the carbon atoms in the  $n$ -alkyl chain, which also increases the hydrophobicity of the copolymers,  $N_{\text{agg}}$  of the copolymers increased. As seen in Table 4  $N_{\text{agg}}$  of the first three entries tend to increase with temperature, which is most profoundly seen for  $\text{EO}_{108}\text{PrGC}_{38}\text{EO}_{108}$ .  $\text{EO}_{108}\text{EtGC}_{38}\text{EO}_{108}$  is the most hydrophilic from the studied copolymers, and as previously shown [21] its ability to self-associate is low. An elevated temperature is required in order to yield only one type of aggregates and therefore to achieve a system suitable for the correct SLS measurements. For the most hydrophobic copolymer

Table 3

Dynamic and static light scattering data for  $\text{EO}_{108}\text{AGC}_{38}\text{EO}_{108}$  aqueous micellar systems at different temperatures

Sample	$T$ (°C)	$R_h$ (nm)	$R_g$ (nm)	$R_g/R_h$
$\text{EO}_{108}\text{EtGC}_{38}\text{EO}_{108}$	25	3.6 <sup>a</sup>	<15	–
	40	5.3	<15	–
	50	6.8	<15	–
	60	7.4	<15	–
$\text{EO}_{108}\text{PrGC}_{38}\text{EO}_{108}$	25	8.4	<15	–
	40	8.6	<15	–
	50	8.7	<15	–
	60	8.7	<15	–
$\text{EO}_{108}\text{BuGC}_{38}\text{EO}_{108}$	25	10.7	<15	–
	40	9.8	15.7	1.60
	50	9.2	16.7	1.82
	60	9.2	17.5	1.90
	70	10.2	16.0	1.60
$\text{EO}_{108}\text{PnGC}_{38}\text{EO}_{108}$	25	13.9	32.3	2.32
	40	12.5	33.9	2.71
	50	11.6	29.3	2.53
	60	12.6	25.9	2.05

<sup>a</sup> Only for the micellar population. For  $\text{EO}_{108}\text{EtGC}_{38}\text{EO}_{108}$  aqueous solution aggregates of  $R_h = 74$  nm were observed [21].

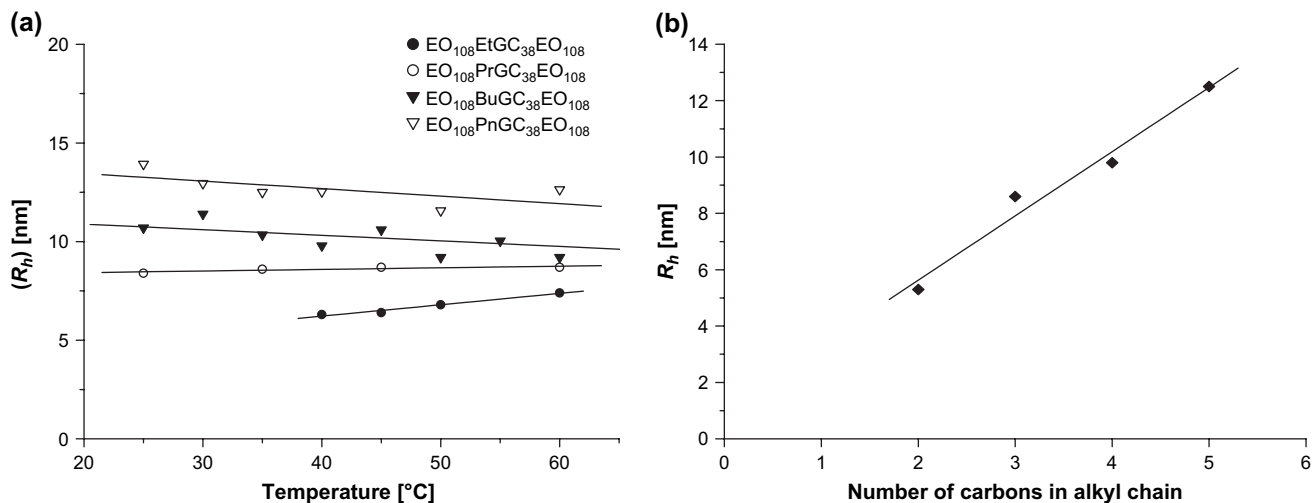


Fig. 5. (a) Temperature dependence of  $R_h$  for  $\text{EO}_{108}\text{AGC}_{38}\text{EO}_{108}$  micelles in aqueous solutions (5 g/L); (b)  $R_h$  at 40 °C as a function of number of carbons in alkyl chain.

$\text{EO}_{108}\text{PnGC}_{38}\text{EO}_{108}$  the molar masses of micelles and their aggregation numbers decrease at 40 °C. There are several possibilities for the temperature-induced change of  $N_{\text{agg}}$ . Previously, it was shown [21] that  $N_{\text{agg}}$  can change as a result of a reorganization within the micellar system leading to changes in the number of micelles which correspond to increasing or decreasing of the  $N_{\text{agg}}$  values, respectively. Sometimes the change of  $N_{\text{agg}}$  can be accompanied by the change of the actual shape of the micelles.

The ratio  $R_g/R_h$  provides information about the particle density and shape [25,26]. Typically  $R_g/R_h$  for spherical micelle with swollen shell equals to 1.3.  $R_g/R_h$  values from 1.6 to 2 can indicate a presence of elongated [27] or thread-like [28] micelles. Values above 2 are typical for rod-like micelles [28].  $R_g/R_h$  data for  $\text{EO}_{108}\text{AGC}_{38}\text{EO}_{108}$  are presented in Table 3.

In the temperature interval from 40 to 70 °C the  $R_g/R_h$  values of micelles of  $\text{EO}_{108}\text{BuGC}_{38}\text{EO}_{108}$  are in the range 1.6–1.9 (except for 25 °C, see above), which most likely corresponds to an elongated shape.

$R_g/R_h$  ratios of micelles from  $\text{EO}_{108}\text{PnGC}_{38}\text{EO}_{108}$  are larger than 2 within the whole investigated temperature interval. The lowest values of  $R_g/R_h$  for  $\text{EO}_{108}\text{PnGC}_{38}\text{EO}_{108}$  are observed at 60 °C, which is just before the cloud point and at such conditions the aggregates tend to become more compact.

The temperature dependence of  $R_g/R_h$  ratios for the micelles of  $\text{EO}_{108}\text{BuGC}_{38}\text{EO}_{108}$  and  $\text{EO}_{108}\text{PnGC}_{38}\text{EO}_{108}$  micelles is presented in Fig. 7. It is clearly seen that the micelles from  $\text{EO}_{108}\text{BuGC}_{38}\text{EO}_{108}$  are of more stable shape, while  $\text{EO}_{108}\text{PnGC}_{38}\text{EO}_{108}$  micelles exhibit pronounced changes in their  $R_g/R_h$  ratio, which has its maximum of 2.71 at 40 °C.

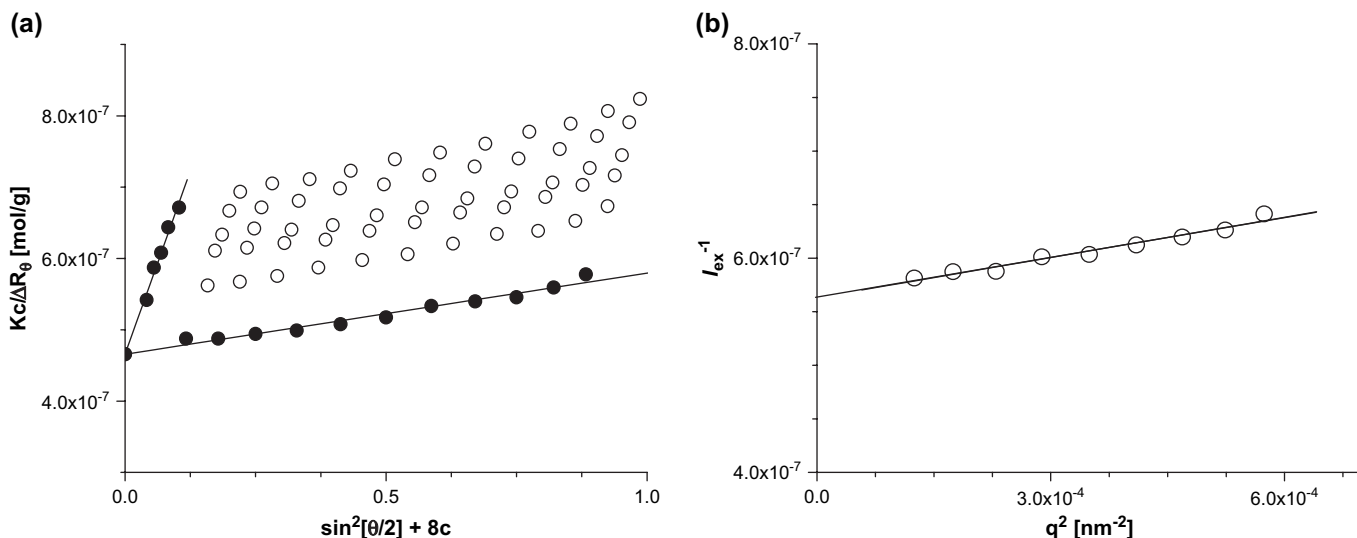


Fig. 6. (a) Zimm plot for  $\text{EO}_{108}\text{PnGC}_{38}\text{EO}_{108}$  at 25 °C; (b) partial Zimm plot for 5 g/L micellar dispersion of  $\text{EO}_{108}\text{PnGC}_{38}\text{EO}_{108}$  at 50 °C.

Table 4  
Molar mass  $M_w$  and aggregation number  $N_{agg}$  for the  $EO_{108}AGC_{38}EO_{108}$  micelles

Sample	$M_w^{uni}$	$M_w^{mic}$ 25 °C	$N_{agg}$ 25 °C	$M_w^{mic}$ 40 °C	$N_{agg}$ 40 °C
$EO_{108}EtGC_{38}EO_{108}$	15 500	—	n.a.	42 000	3
$EO_{108}PrGC_{38}EO_{108}$	15 200	264 000	17	311 000	20
$EO_{108}BuGC_{38}EO_{108}$	15 700	649 000	41	825 000	53
$EO_{108}PnGC_{38}EO_{108}$	16 200	2 150 000	132	1 650 000	102

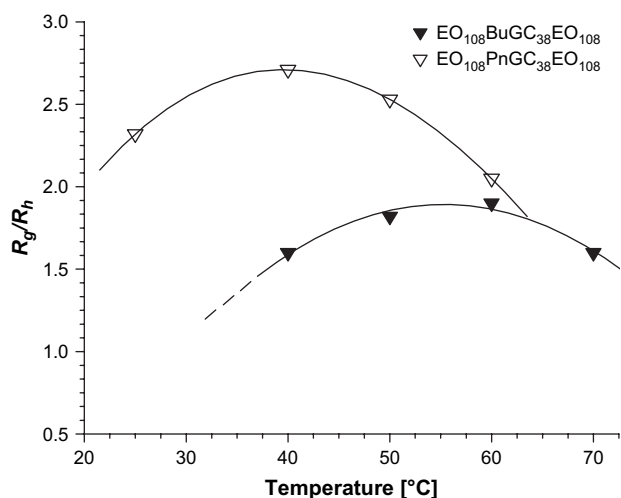


Fig. 7.  $R_g/R_h$  versus temperature for  $EO_{108}BuGC_{38}EO_{108}$  (black triangles) and  $EO_{108}PnGC_{38}EO_{108}$  (hollow triangles).

It was not possible to determine the  $R_g$  values for micelles from  $EO_{108}EtGC_{38}EO_{108}$  and  $EO_{108}PrGC_{38}EO_{108}$ , as at all of the investigated temperatures the radii of gyration were smaller than 15 nm, which is the lower limit of the static light scattering measurements (isotropic scatterer). Nevertheless the most probable shape of the micelles from the latter two copolymers is expected to be spherical, mostly due to the low  $N_{agg}$  values (Table 4).

Light scattering techniques are not powerful enough to ultimately confirm the micellar size distribution and the exact shape within a given system. Other methods, in particular cryo-TEM, should be used in parallel for this purpose. However, the combination of SLS and DLS and the respective  $R_g/R_h$  values yields at least a descriptive information about the average shape of the studied micelles.

#### 4. Conclusions

The length of *n*-alkyl chain incorporated into glycidyl units of  $EO_{108}AGC_{38}EO_{108}$  block copolymers plays an important role in their self-association behaviour in aqueous media. Results of the study of new and well defined  $EO_{108}AGC_{38}EO_{108}$  amphiphilic block copolymers possessing the same backbone, and differing only by the *n*-alkyl group in the alkyl glycidyl carbamate units in the middle block show that the hydrophobicity of incorporated compounds is the dominant factor on the cloud point values, cmc values, hydrodynamic radii,

radii of gyration, molar masses of micelles and their aggregation numbers. The increasing number of carbons in alkyl chain of the central hydrophobic block (increased hydrophobicity) causes a decrease in the observed cloud point temperature and in the cmc value. In the case of hydrodynamic radii, radii of gyration, molar masses of micelles and their aggregation numbers, determined using dynamic and static light scattering technique, the influence of the length of alkyl chain present in middle block of  $EO_{108}AGC_{38}EO_{108}$  copolymers is opposite – with increasing number of carbons in alkyl chain the values of all these parameters increased.

The relative hydrophobicity of  $EO_{108}AGC_{38}EO_{108}$  copolymers plays an important role in the composition–supramolecular morphology relationship. Micelles from the first two homologs  $EO_{108}EtGC_{38}EO_{108}$  and  $EO_{108}PrGC_{38}EO_{108}$  are presumably of spherical shape due to the low aggregation numbers observed. More hydrophobic copolymers  $EO_{108}BuGC_{38}EO_{108}$  and  $EO_{108}PnGC_{38}EO_{108}$  seem to aggregate into elongated and rod-like micellar structures.

#### Acknowledgements

This work was supported by European Commission project “NANOSTIM”, MTKD-CT-2004-509841 and by the Polish Ministry of Education and Science, grant no. 4 T09A 052 25. One of the authors (M.J.-P.) appreciates the fellowship granted by Regional Fund of the Ph.D. Scholarships.

#### References

- [1] Gohy J-F. Adv Polym Sci 2005;190:65.
- [2] Kita-Tokarczyk K, Grumelard J, Haelele T, Meier W. Polymer 2005;46:3540.
- [3] Mortensen K. J Phys Condens Matter 1996;A103:8.
- [4] Savic R, Eisenberg A, Maysinger D. J Drug Target 2006;14(6):343.
- [5] Bronstein L, Kramer E, Berton B, Burger C, Foerster S, Antonietti M. Chem Mater 1999;11:1402.
- [6] Aizawa M, Buriak JM. J Am Chem Soc 2006;128:5877.
- [7] Gil ES, Hudson SM. Prog Polym Sci 2004;29:1173.
- [8] Riess G. Prog Polym Sci 2003;28:1107.
- [9] Booth C, Attwood D. Macromol Rapid Commun 2000;21:501.
- [10] Mingvanish W, Mai SM, Heatley F, Booth C, Attwood D. J Phys Chem 2003;103:767.
- [11] Yuan J, Li Y, Li X, Cheng S, Jiang L, Feng L, et al. Eur Polym J 2003;39:767.
- [12] Yu Y, Eisenberg A. J Am Chem Soc 1997;119:8383.
- [13] Liu T, Zhou Z, Wu Ch, Chu B, Schneider DK, Nace VN. J Phys Chem 1997;101:8808.
- [14] Alexandridis P, Holzwarth JF, Hatton TA. Macromolecules 1994;27:2414.
- [15] Yang YW, Deng NJ, Yu G-E, Zhou ZK, Attwood D, Booth C. Langmuir 1995;11:4703.
- [16] Kataoka K, Kwon GS, Yokoyama M, Okano T, Sakurai Y. J Control Release 1993;24:119.
- [17] Osada K, Kataoka K. Adv Polym Sci 2006;202:113.
- [18] Liu T, Zhou Z, Wu Ch, Nace VM, Chu B. J Phys Chem B 1998;102:2875.
- [19] Alexandridis P, Hatton TA. Colloids Surf A 1995;96:1.
- [20] Fitton A, Hill J, Jane D, Miller R. Synthesis 1987;1140.
- [21] Dimitrov Ph, Utrata-Wesołek A, Rangelov S, Wałach W, Trzebicka B, Dworak A. Polymer 2006;47:4905.



- [22] Hiemenz PZ. Principle of colloid and surface chemistry. New York: Marcel Dekker Inc.; 1985.
- [23] Yu G-E, Altinok H, Nixon SK, Booth C, Alexandridis P, Hatton T. Eur Polym J 1997;33:613.
- [24] Grant CD, Steege KE, Bunagan MR, Castner Jr EW. J Phys Chem B 2005;109:22273.
- [25] Thurn A, Burchard W, Niki R. Colloid Polym Sci 1987;265:653.
- [26] Burchard W. Adv Polym Sci 1983;48:1.
- [27] Dimitrov Ph, Porjazoska A, Novakov ChP, Cvetkovska M, Tsvetanov ChB. Polymer 2005;46:6820.
- [28] Zhou Z, Yang YW, Booth C, Chu B. Macromolecules 1996;29:8357.